JOURNAL OF GEOPHYSICAL RESEARCH, VOL. 102, NO. B8, PAGES 18,391–18,403, AUGUST 10, 1997

Spectral analyses of the KTB sonic and density logs using robust nonparametric methods

Alan G. Jones
Geological Survey of Canada, Ottawa, Ontario

Klaus Holliger
Institute of Geophysics, Swiss Federal Institute of Technology, ETH-Hönggerberg, Zurich, Switzerland

Abstract. We use robust techniques to estimate power spectra, coherences and transfer functions of the German Continental Deep Drilling Program (KTB) sonic and density logs and lithologically defined subsets thereof. Our results confirm the overall 1/wavelength-decay of the power spectra inferred by parametric analyses, but provide superior resolution and nonparametric estimates of errors and statistical significance. We demonstrate the absence of any statistically meaningful coherence between the velocity logs from the main and pilot holes, suggesting a spatially quasi-isotropic upper crustal velocity structure. Also, there is little coherence between the physical and caliper logs, indicating that disturbances introduced by breakouts and uneven relief of the borehole wall mostly contribute to the uncorrelated portions of the velocity logs. Coherence between the gamma and physical logs is weak to absent, indicating that the observed velocity and density fluctuations are dominated by the physical state of the rocks rather than by their petrological composition. Attempts to derive Poisson's ratio, and its variation with wavelength, from the relationship between the shear and compressional velocity logs met with limited success, but imply that caution should be exercised when comparing Poisson's ratio derived from laboratory studies on samples representative of a region to crustal-scale seismic determinations. Our preferred interpretation is that fluctuations in the physical logs in the intermediate wavelength range (~10-150 m) are dominated by cracks and their level of fluid saturation. At larger wavelengths (>50-150 m) the effects of the petrology becomes more significant as shown by changes in slope of the power spectra and the emerging coherence between the *Vp* and the gamma logs.

Introduction

Densities and seismic velocities contain information on the petrology and physical state of the Earth's interior. Inferences about velocity and density distributions are made through modeling and inversion of seismic and gravimetric data, or by laboratory measurements on rock samples considered representative of certain localities and depth ranges. In the upper 10 km of the Earth's crust the gap in information obtained from low-resolution surface measurements, and from well-defined, but spatially aliased, laboratory measurements, can be bridged by borehole measurements and the analyses of borehole logs.

Traditionally, deep boreholes (1000 m or deeper) in crystalline rocks were drilled exclusively for purposes of mineral exploration and, if logging was undertaken at all, only electrical logs were run [e.g., *Dyck*, 1975]. Since the early 1980s, deep continental drilling has been initiated for research on nuclear waste storage [e.g., *Green and Mair*, 1983] and for scientific purposes [e.g., *Silver and James*, 1988]. Moreover, recent studies combining sonic and density log information with high-resolution seismic reflection data have shown promise for mineral exploration and civil engineering purposes [e.g., *Milkereit et al.*, 1994].

In both sedimentary and crystalline rocks, velocity and density logs are characterized by strong local variability far in excess of their large-wavelength trends, which favors a stochastic, rather than a deterministic, approach to interpretation. In order to understand phase and amplitude distortions of seismic waves and to improve prediction filters, considerable effort has been made to discern the statistical properties of velocity and density logs in sedimentary environments [e.g., *Walden and Hosken*, 1985; *Todoeschuck and Jensen*, 1988]. Comparable studies from crystalline rocks are, however, still in their infancy, and the majority of these studies have been carried out on logs from the ultradeep German Continental Deep Drilling Program (*Kontinentales Tiefbohrprogramm*, henceforth referred to as KTB) [*Wu et al.*, 1994; *Kneib*, 1995; *Holliger*, 1996a].

All of the studies cited above followed the classical parametric approach for estimating the second-order statistics of time (or space) series data [e.g., *Bendat and Piersol*, 1971, pp. 322-330; *Brillinger*, 1981, Chapter 5]: after removing a more-or-less arbitrarily chosen deterministic component, the power spectra and/or autocovariance functions of the logs are calculated and interpreted according to some (preconceived)

Paper number 96JB03668.
0148-0227/97/96JB-03668$09.00

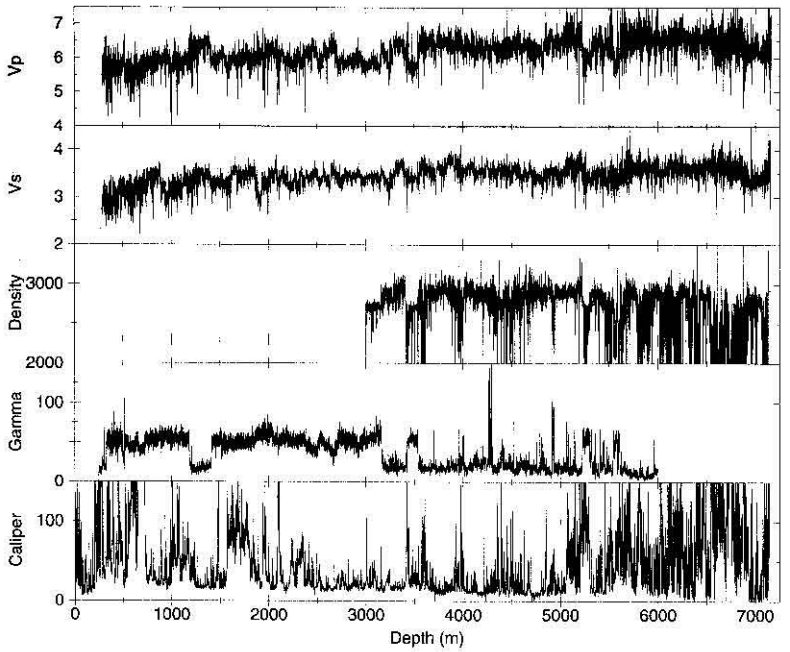

Figure 1. Plot of the five logs for the pilot hole. *Vp* log (in *km/s*), *Vs* log (in *km/s*), density log (in kg/m^3), gamma log (in counts), and caliper log (in *mm*).

parametric model. Such global estimates of the second-order statistics may, for example, be useful for constraining random seismic models [e.g., *Holliger*, 1997]. However, owing to the generally poor resolution, little can be learned about the origin of the density and velocity heterogeneity in the upper crystalline crust.

In this paper we attempt to overcome this limitation by using robust, nonparametric, spectral methods (see reviews by *Huber* [1981], *Hoaglin et al.* [1983], *Hampel et al.* [1986], *Thomson and Chave* [1991]. In addition to the full logs we also analyze subsets of the logs defined petrologically by the approximately bimodal rock column penetrated by the KTB boreholes. The aim of our study is to obtain well-constrained and well-resolved estimates of power spectra and coherences, and their errors, from the KTB logs in order to explore the origins of their small-scale variability. We follow the approach described in detail in *Chave et al.* [1987], to which the reader is referred for a complete mathematical treatment of the robust estimation of power spectra, coherences, and transfer functions.

KTB Logs

Data and Data Subsets

The two KTB boreholes in southeastern Germany are located some 200 m apart and reach to depths of about 4000 m for the pilot hole ("Vorbohrung" or VB) and 9000 m for the main hole ("Hauptbohrung" or HB). The logs for each hole considered in this study are the *P* wave velocity (*Vp*) sonic log, the *S* wave velocity (*Vs*) sonic log, the density log, the gamma log, and the caliper log (Figures 1 and 2). The caliper logs were obtained by taking the two perpendicular caliper measurements, averaging them, and subtracting the reference borehole diameter. The pilot hole has complete logs, from 65 m to about 4000 m. For the main hole, sonic logs reaching from 285 to 7160 m were available to us. Density logging was not undertaken in the main hole at depths shallower than 3003 m, and our gamma log is complete only to about 6000 m. All logs were acquired with a sampling interval of 0.152 m (6 inches).

Both boreholes penetrate steeply dipping amphibolite-facies, intermediate paragneisses interlayered with metabasites [*Franke*, 1989]. Radiometric age dating indicates an early to middle Variscan (320-380 Ma) peak of metamorphism for both the paragneisses and the mafic rocks [*Hansen et al.*, 1989]. This bimodal petrology is clearly reflected in the gamma logs: in the pilot hole, gamma counts are around 100 for the paragneisses and around 25 for the metabasites, whereas for the main hole these counts are 55 and 20, respectively. On the basis of the gamma logs, the sonic and density logs from both holes were partitioned into two sets: set G (gneiss) and set M (metabasite). Depth intervals for the pilot and main holes are given in Tables 1 and 2, respectively. Regions outside the defined depth intervals were excluded from detailed spectral analysis due to insufficient data quality of the gamma and/or density logs. Note that although the main hole is far deeper than the pilot hole, the maximum depths for our subsets are almost the same, at 4262 m and 3965 m, respectively.

Figure 3 displays histograms of *Vp* (Figure 3a), *Vs* (Figure 3b) and density (Figure 3c) for the two sets independently, and for both logs combined. Subsets G and M both display Gaussian-like distributions in all three parameters, but differ significantly in terms of their average *Vp* and density values. In contrast, there is not a strong difference in distributions of *Vs* values for the two subsets. Since the cumulative distributions of the full logs are also Gaussian-like, as shown by the dashed lines in Figure 3 and previously discussed by *Wu et al.* [1994], *Kneib* [1995], and *Holliger* [1996a], the fundamental bimodal nature of the distribution of *Vp* and density is obscured. The interrelationships between the lithologically defined subsets for the three physical logs are illustrated in Figure 4. Gneisses appear to have little density variation but compressional wave velocity variation ranging from 5250 to 6250 m/s (Figure 4,

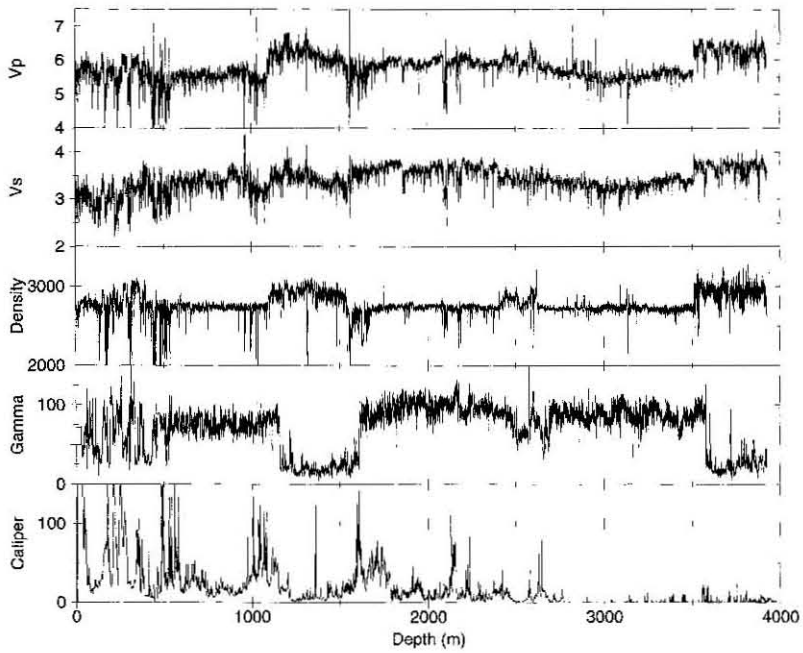

Figure 2. Plot of the five logs for the main hole. *Vp* log (in *km/s*), *Vs* log (in *km/s*), density log (in kg/m^3), gamma log (in counts), and caliper log (in *mm*).

left). The relation between *Vp* and *Vs* is more pronounced in metabasites than in paragneisses (Figure 4, middle). This illustrates importance of not only considering the full logs but also analyzing lithologically-defined subsets thereof.

Previous Work

Wu et al. [1994] subtracted a linear trend from the KTB *Vp* logs and analyzed the power spectra of the residual data series. They concluded that the power spectra of both holes decayed approximately as 1/wavenumber over scales ranging from about 1 m to more than 1000 m. Modeling the correlation between the *Vp* logs from the pilot and main holes, *Wu et al.* [1994] inferred an aspect ratio (horizontal/vertical correlation scale) of 2 to 3. *Kneib* [1995] subdivided the *Vp*, *Vs*, and density and logs of the main hole into 244-m-long subsets (this window length was chosen arbitrarily), calculated autocovariance functions of these subsets, and summed these local estimates to obtain global estimates for the entire logs. The resulting global autocovariance functions were modeled as the superposition of two exponential autocovariance functions with correlation scales of 1 and 20 m. *Holliger* [1996a] estimated the second-order statistics of the *Vp* logs of the main and pilot holes including the effects of a deterministic velocity component, the system response of the logging process, and noise. The results obtained are compatible with those of *Wu et al.* [1994], apart from suggesting a much shorter range (<200 m) of validity of the 1/wavenumber decay of the power spectrum. Holliger [1996a] also showed that *Kneib*'s [1995] superposition of two exponential autocovariance functions is equivalent to a power spectrum decaying approximately as 1/wavenumber in the range from 1-2 m to 30-40 m. Deviations of this 1/wavenumber decay at smaller (<1-2 m) and larger (30-40 m) scales are likely due to the inherent averaging of the logging procedure and the maximum wavelength present in the subsets (determined by the length of the data window), respectively [*Holliger*, 1996a].

Table 1. Depth Intervals for the Subset Division of the Pilot Hole (VB)

Set	Depth Interval (m)	Number of Data Points
G1V	520-1160	4200
M1V	1160-1610	2954
G2V	1610-2470	5644
M2V	2470-2691	1451
G3V	2691-3575	5800
M3V	3575-3985	2691

The gneiss sequences start with set name G, and the metabasites start with set name M.

Table 2. Depth Intervals for the Subset Division of the Main Hole (HB)

Set	Depth Interval (m)	Number of Data
G1H	731-1182	2959
M1H	1182-1410	1496
G2H	1410-2386	6405
M2H	2386-2709	2119
3H	2709-3161	2966
M3H	3161-3427	1745
G4H	3427-3532	689
M4H	3532-4262	4790

The gneiss sequences start with set name G, and the metabasites start with set name M.

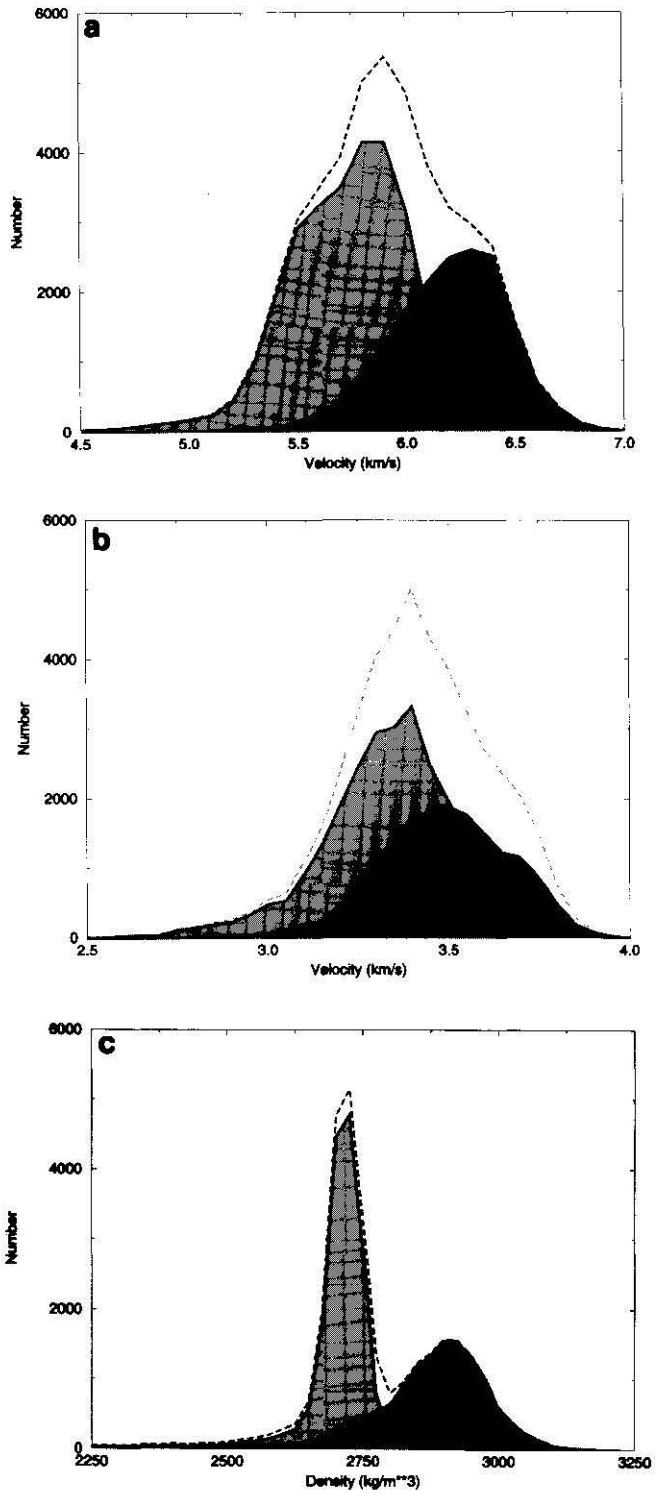

Figure 3. Histograms of the data from the three physical logs from both holes (dashed lines), and from the gneiss (set G, light gray) and metabasite (set M, dark gray) subsets listed in Tables 1 and 2. (a) *Vp* logs, (b) *Vs* logs, and (c) density logs.

Robust Spectral Analysis of Noisy, Non-Gaussian Data

Obtaining information about the scaling relationships of crustal heterogeneity from spectral analyses of well log data must be undertaken with care. Previous spectral examinations of KTB logs utilized standard methods, with Fourier transformation of the data after removing a deterministic trend and applying some form of smoothing window to taper the ends of the data series [Wu et al., 1994]. With the exception of detrending [*Owens*, 1978], such approaches theoretically yield accurate estimates of the spectra, after correction for the form of the window [*Jenkins and Watts*, 1968, pp. 230-233]. In practice, however, geophysical data rarely conform to the ideal statistical nature required by these methods, such as stationarity and Gaussian distributions of both data and noise. Geophysical data almost always contain non-Gaussian noise and are locally nonstationary, which, even as a small fraction of the total data, can severely influence, and even overwhelm, conventional statistical estimates in a manner that is both unpredictable and undetectable. Two of the most typical problems are data outliers and local nonstationarity, and if these exist in a data series, then the resulting spectra in the frequency domain will be poorly estimated by standard parametric methods [*Chave et al.*, 1987]. These problems have been addressed by data conditioning procedures, such as median filtering. However, this leads to unpredictable nonlinear spectral distortion and hence must be avoided when investigating detailed spectral behavior.

Robust methods for data analysis have been advanced over almost three decades, principally to address the problems of data outliers and local nonstationarity (see reviews by *Huber* [1981], *Hoaglin et al.* [1983], *Hampel et al.* [1986], and *Thomson and Chave* [1991]). Estimation of parameters using least squares procedures is highly unstable in the presence of even a small number of outliers, as they can exert undue influence on the estimation of the parameters. As an example, consider a problem of deriving the relationship between two variables, x and y, from a set with 41 error-free data lying in the bounds x=[-1,1] and y=[-1,1] and a single point outlier at $\{x,y\}$= {10,20}, from the process y=x. With standard least squares regression [e.g. *Bendat and Piersol*, 1971, pp. 129-133; *Brillinger*, 1981, pp. 188-192], that outlier has a weight of 100 times the weights of the other points, which results in a least squares estimate of slope of 1.872±0.05, rather than unity, with an intercept of 0.031±0.087, rather than zero. Examination of the residuals does not indicate a problem with this regression, as the outlier's residual is 1.25, whereas those of the points close to the bounds are 0.8-0.9. Also the correlation coefficient is misleadingly high at 0.984. Obviously, in this case one could argue that the outlier would have been rejected after visual scrutiny of the data, but for large and complex datasets such scrutiny is, at best, impractical, and, more realistically, impossible. In contrast, robust methods of parameter estimation are far less sensitive to the presence of a moderate amount of data that are either "bad" or do not conform to the model characterizing the majority of the data. Undertaking a robust linear regression analysis of the above data set following the scheme outlined in *Huber* [1981, p. 18; c=1.5, 250 iterations], the slope and intercept estimates are 1.0081±0.0002 and 0.0010 ±0.00036, respectively, with a correlation coefficient of 0.9999991.

For spectra estimation, *Thomson* [1977a, b] showed that outliers are a serious problem, even for long data series. As coherences and transfer functions are derived from products and ratios of auto- and cross-spectra from multiple data series, they are even more susceptible to distortion than the spectral estimates themselves. Robust spectral analysis methods

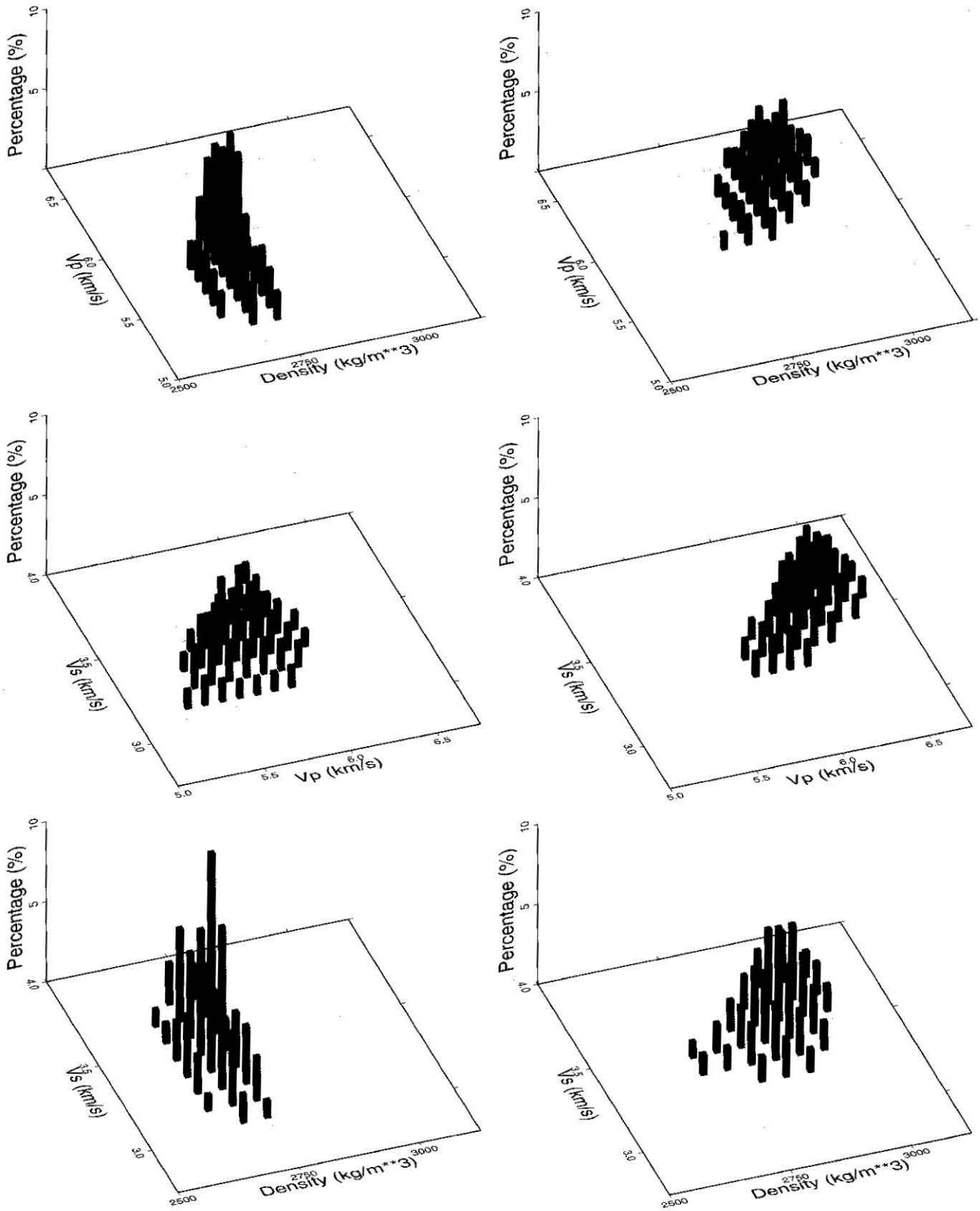

Figure 4. Comparison of the interrelationships between the three physical logs for the (left) gneiss and (right) metabasite subsets. (top) Density-*Vp*; (middle) *Vp*-*Vs*; (bottom) density-*Vs*.

advanced during the last two decades, principally in telecommunications, have found their way into the geophysical literature, particularly in the processing of magnetotelluric time series [*Jones and Jödicke*, 1984; *Egbert and Booker*, 1986; *Chave et al.*, 1987; *Chave and Thomson*, 1989; *Jones et al.*, 1989; *Thomson and Chave*, 1991]. A striking example of the difference between standard cross-spectral methods and robust methods for transfer function estimation is given by *Jones et al.* [1989], whose comparison of eight different methods illustrates that weak signals can be extracted from noise using one of the three robust methods, whereas the five standard methods performed poorly. In the following, we use such robust methods to analyze the spectral properties of the KTB sonic and density logs. Error estimates are derived using the nonparametric jackknife approach [*Efron*, 1982], which is vastly more reliable and accurate than parametric approaches [*Thomson and Chave*, 1991]. The mathematics used in our analysis is entirely based on *Chave et al.* [1987], to which the interested reader is referred, and will not be reiterated here.

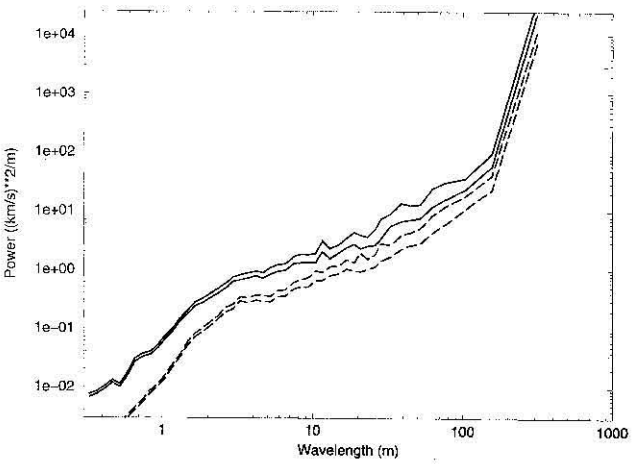

Figure 6. Power spectra from the pilot and main boreholes for the *Vp* and *Vs* logs. Shown are the 95% confidence intervals for the estimates of the *Vp* power spectra (solid lines) and *Vs* power spectra (dashed lines).

Robust Power Spectra

The robust estimation procedures for power spectra advocated by *Chave et al.* [1987] use a variant of maximum likelihood, the M-estimator, over the alternative L-estimator, deemed useful for location problems, as the latter require a priori information to specify the truncation point and hence is not data adaptive. The methodology is described in detail in *Chave et al.* [1987, pp. 639-641, Eqns. 21, 23, 27]. The robust spectra have been derived after applying third-order autoregressive prewhitening to the original data, then applying a prolate-spheroidal data taper window [*Slepian*, 1978], with a space-bandwidth product of one to each data section. The latter is a low-bias data window superior to the standard cosine bell (Hanning window) but with similar resolution characteristics [*Thomson*, 1982].

A comparison of conventional spectrum estimation with robust spectrum estimation for the *Vp* log from the main hole is shown in Figure 5. The conventional power spectrum, derived using fast Fourier transformation after Parzen window conditioning to reduce leakage [*Bendat and Piersol*, 1971, pp. 319-320], exhibits more than a decade of scatter in the estimates. In comparison, the robust power spectrum [*Chave et al.*, 1987, pp. 639-641], together with the 95% confidence limits determined using the jackknife [*Thomson and Chave*, 1991], is far smoother and the errors are typically less than 1/10 of a decade, except for long wavelengths. Clearly, if one wishes to estimate the spectral slope, then one can accomplish this with superior statistical confidence using robust estimates rather than conventional ones.

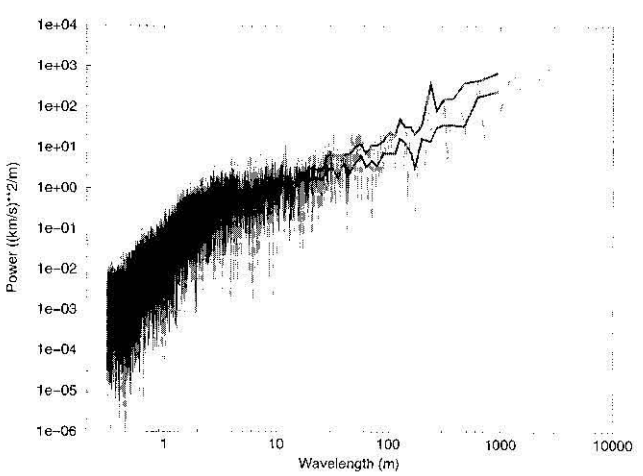

Figure 5. Comparison of conventional power spectrum estimation (thin line) with robust spectrum estimation (thick gray line), plus 95% confidence intervals (thinner gray lines), for the *Vp* log from the main hole.

The robust power spectra of the *Vp* and *Vs* logs from the two holes combined are shown in Figure 6. Both spectra show a well-defined linear region for wavelengths of 3-150 m. The slopes of the spectra both increase significantly for wavelengths shorter than 3 m and wavelengths longer than 150 m. These changes in slope are consistent with the logging system response at short wavelengths and the outer scale of self-affine behavior at longer wavelengths inferred by *Holliger* [1996a]. Linear regression analyses [e.g. *Bendat and Piersol*, 1971, pp. 129-133; *Brillinger*, 1981, pp. 188-192] of the spectra in the region 3-150 m show that they are well described by a linear function in double logarithmic space, with correlation coefficients of 0.98 for both *Vp* and *Vs*. The slopes of the two regressions are 1.11±0.04 and 1.18±0.04 for *Vp* and *Vs*, respectively. The slope for the *Vp* log is not statistically close to the values of 0.97 ± 0.005 for the main hole and 1.25 ± 0.004 for the pilot hole quoted by *Wu et al.* [1994]. This discrepancy could be due to the averaging of the logs, and is explored below. Another indicator of statistical confidence can be obtained from applying linear regressions to the 95% confidence curves, which yields slopes of 1.05-1.18 for *Vp* and 1.06-1.19 for *Vs*, with errors of order ±0.05 to ±0.06.

Separate sonic log spectra for the two lithologically defined subsets G and M are plotted in Figure 7a for the pilot hole and in Figure 7b for the main hole. The *Vp* spectra from the logs for the two sets in either borehole are very similar in the wavelength range of 3-100 m; however, they differ between the two holes. This difference is shown in Figure 8a for the spectra from the two *Vp* logs. There is a difference, at the 95% confidence level, between the spectra in the wavelength range 1.5-10 m. For other wavelengths, the two spectra are within each other's 95% confidence bounds. In contrast, the spectra from the *Vs* logs are statistically indistinguishable over the

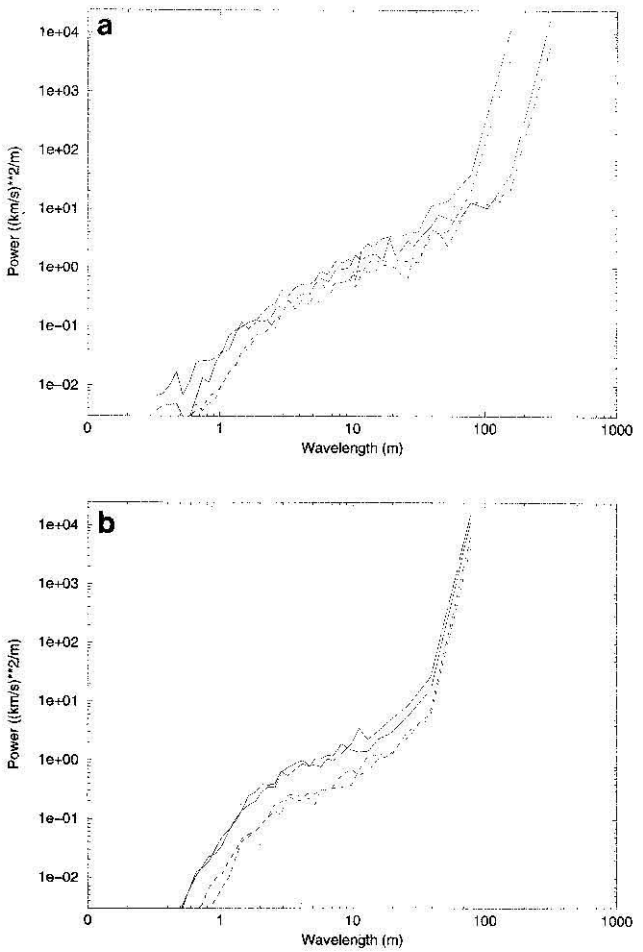

Figure 7. Comparison of the *Vp* (solid lines) and *Vs* (dashed lines) power spectra from the gneiss and metabasite subsets (see Tables 1 and 2) from the logs for the (a) pilot and (b) main holes.

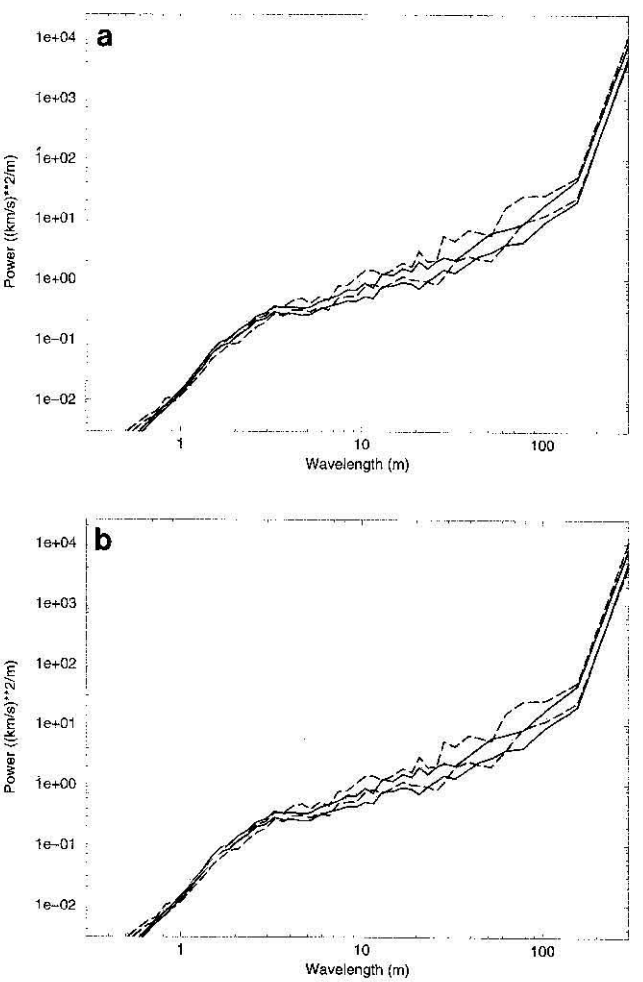

Figure 8. Comparison of the velocity spectra from the logs of the pilot (dashed lines) and main (solid lines) holes. The lines are the 95% confidence intervals of the means: (a) *Vp* spectra and (b) *Vs* spectra. Note that whereas the *Vs* spectra from the two holes are statistically identical, the *Vp* spectra show a marked difference in the 2-6 m wavelength range.

entire wavelength range (Figure 8b). The slope estimates from the spectra and from the lower and upper 95% confidence estimates are given in Table 3. Standard errors for all slope estimates are 0.05-0.06. The estimates in Table 3 suggest that there is a statistically significant difference for wavelengths smaller than 10 m between the two holes from the *Vp* logs, but not from the *Vs* logs. In fact, the main hole *Vp* spectra are better fit with two linear regressions, one for the wavelength range of 1.5-10 m, and another for the range 10-150 m, with slopes of 1.75 and 1.34, respectively. As expected from the comparison in Figure 8a, this latter slope is in agreement with the value from the pilot hole *Vp* log. Whether this change in slope at short wavelengths corresponds to a difference in velocity structure between the main and pilot holes or whether it is due to unknown differences in data acquisition and/or data conditioning cannot be decided based on the available information. Given that this change in slope is only found in one of the logs, we tend to favor the second option.

Coherences and Transfer Functions

In an ideal elastic medium, *Vp*, *Vs*, and density are interrelated through elastic constants. Our goal is to study the variation with wavelength of these interrelationships in order to answer the following questions: How are the physical parameters related to the petrology of the probed lithologies?, How are the log measurements affected by breakouts and irregular relief of the borehole wall? To this end, we have analyzed the logs for interlog and interhole coherence in the wavenumber domain. Coherence is the magnitude-squared coherency between two data series, where coherency is the complex-valued frequency- or wavenumber-domain analogue of the coefficient of cross-correlation [*Jenkins and Watts*, 1968, pp. 351-353; *Brillinger*, 1911, pp. 256-257]. To determine how statistically significant the estimates of coherence are, we also

Table 3. Linear Regressions to the *Vp* and *Vs* Spectra and Their 95% Confidence Intervals From the Pilot (VB) and Main (HB) Holes

Hole and Log	Slope	Lower 95%	Upper 95%
VB *Vp*	1.28	1.15	1.40
HB *Vp*	1.04	0.97	1.11
VB *Vs*	1.17	1.05	1.28
HB *Vs*	1.09	1.01	1.16

compute the expectation value for the estimate of coherence between two completely uncorrelated data series. Whereas the expectation value of coherence between such two data series is zero, the expectation of the estimate of coherence is non-zero due to inherent bias, and its value is inversely proportional to the number of degrees of freedom [*Nuttall and Carter*, 1976; *Jones*, 1979; *Chave et al.*, 1987]. Accordingly, this bias increases with increasing wavelength as the number of available estimates decreases. An equivalent bias also occurs for estimation of cross-correlation coefficients [e.g., *Bendat and Piersol*, 1971, pp. 126-128]. The robust estimation of coherence is described in *Chave et al.* [1987, p. 643, Eqns. 34-36].

Interlog Coherence

Coherence measurements between the physical logs and caliper logs contain information on variations of the dependence of the former on the relief of the borehole wall and thus may allow us to identify and eliminate artifacts. Our analyses indicate that for both boreholes there is generally no statistically significant coherence between the physical and caliper logs. The sole exception is the caliper and density logs of the gneiss sequences in the pilot hole, which show a reasonable coherence at the 0.4-0.5 level. This implies that the effects of breakouts and uneven borehole wall relief on the density and sonic logs are largely uncorrelated and hence only affect the white, or quasi-white, part of the log spectra. This result is consistent with that of *Holliger et al.* [1996], who found that for the Stenberg borehole (central Sweden) the local variance of caliper fluctuations and the local variance of white noise present in the sonic log data were closely related.

The coherence between the physical logs and the gamma logs is indicative of how the seismic velocities and densities are related to the petrology of the rock column (Figure 9). The only statistically significant interlog coherence found was between gamma and *Vp* logs at wavelengths longer than 50 m, and it was weak (0.1 - 0.2). Detailed study showed that the

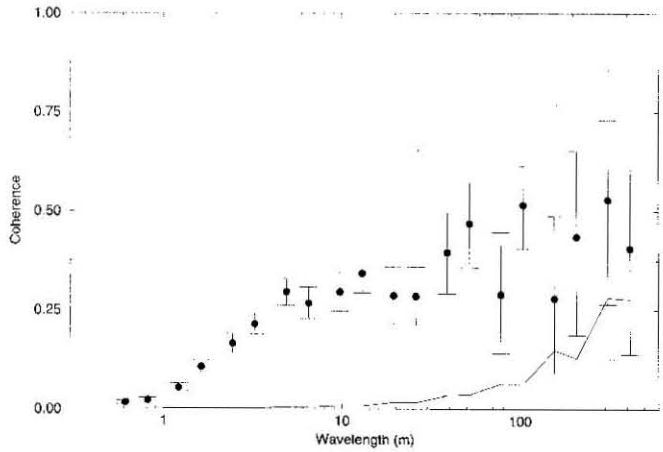

Figure 10. Coherence between the *Vs* and *Vp* logs for both holes as a function of wavelength (inversely proportional to wavenumber). The error bars are 95% confidence intervals, and the solid line is the 95% confidence interval for two incoherent series.

gneiss sequences do not contribute to this coherence. This demonstrates that the sonic and density logs are largely independent of the petrology of the probed rock column. It is conceivable that the emerging coherence between *Vp* and gamma logs, and the changes in slope of the power spectra of the physical logs at larger wavelengths, are related to each other (Figs. 5 to 8). This could indicate that in the short to intermediate wavelength range, density and velocity fluctuations are dominated by the physical state rather than by the petrology, and that the latter only comes into effect at larger wavelengths. It could also indicate that the relatively uniform correlation scales (~60-160 m) of upper crustal sonic logs [*Holliger*, 1996a] are related to this transition from a dominantly physically controlled to a more petrologically controlled seismic structure.

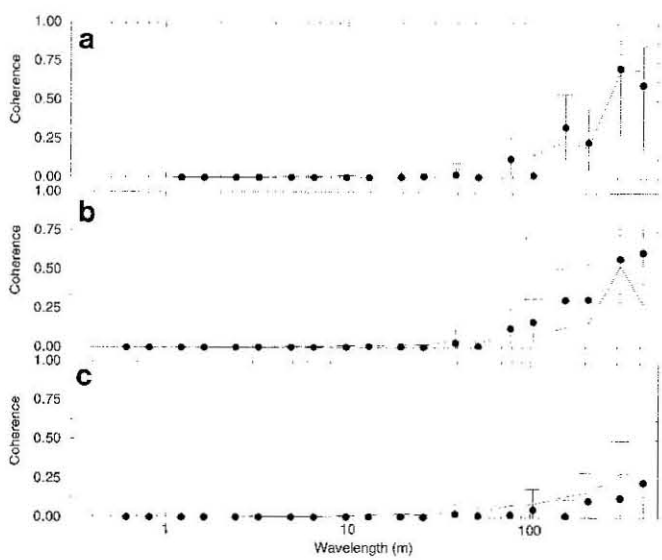

Figure 9. Coherence between the gamma logs and the physical logs: (a) gamma-density, (b) gamma-*Vp*, and (c) gamma-*Vs*. The error bars are 95% confidence intervals, and the solid lines are the 95% confidence interval for two incoherent series.

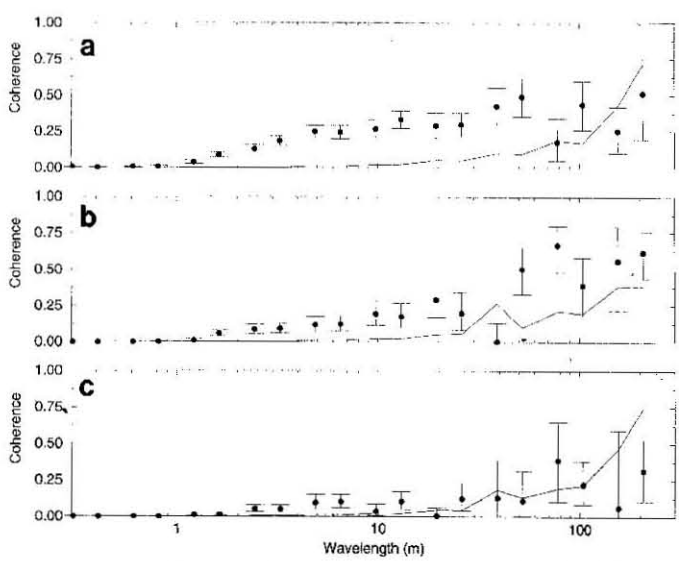

Figure 11. Coherences between the three physical logs from the pilot hole: (a) *Vs*-*Vp*, (b) *Vp*-density, and (c) *Vs*-density. The error bars are 95% confidence intervals, and the solid line is the 95% confidence interval for two incoherent series.

Figure 10 shows the coherence between the *Vs* and *Vp* logs for both holes simultaneously. Coherence is generally stable but uniformly low at around 0.25 for wavelengths of 4.5-150 m. For shorter wavelengths, the coherence drops rapidly, and for wavelengths shorter than 2 m the two logs are incoherent with each other. At long wavelengths the coherence appears to rise, but this statement cannot be defended statistically as the estimate for two uncorrelated sequences also rises rapidly because the number of degrees of freedom decreases. Coherence determinations for the logs separately indicate that overall the *Vs-Vp* coherence is greater in the pilot hole than in the main hole.

The coherences between the three physical logs for the pilot hole are shown in Figure 11 (this is not done for the main hole as the density data are not complete for that hole). Clearly, the density and *Vs* logs are incoherent with each other (Figure 11c), and the values are what one would expect for two uncorrelated series. The two velocity logs are most coherent (Figure 11a), with values of 0.25-0.5 over 4-100 m, whereas the density-*Vp* coherence (Figure 11b) is low at short wavelengths but increases to large values (>0.5) at wavelengths longer than 50 m.

Subset Coherence

The logs can be examined in terms of their subsets to identify differing coherence characteristics between the paragneiss (**G**) and metabasite (**M**) sequences. Perhaps not surprisingly, given the differences shown in Figure 4, the *Vs-Vp* coherence is far higher for the metabasite sequences than for the gneisses (Figure 12). The gneisses exhibit a coherence between the *Vs* and *Vp* sonic logs of around 0.25 in the 5 to 60 m wavelength range (Figure 12a). In contrast, the metabasites show a coherence of 0.45-0.55 in the 5 to 30 m wavelength range, increasing to around 0.8 for longer wavelengths (Figure 12b). The coherence between the density and *Vp* logs (pilot hole logs only) also display a marked difference between the gneiss and metabasite sequences. The density log is incoherent with the *Vp* log for the gneisses (Figure 13a), with values close to the expectation value for two uncorrelated series, whereas for the metabasites there is good coherence starting at wavelengths of 2.5 m. Similarly, the density-*Vs* coherences (not shown) show that the logs from the gneiss sequences are incoherent, whereas for the metabasite sequences there is a resolvable coherence above the 95% confidence interval for incoherent series around 0.2-0.3. This difference suggests that the measured density variations in the gneisses do not correlate with the measured

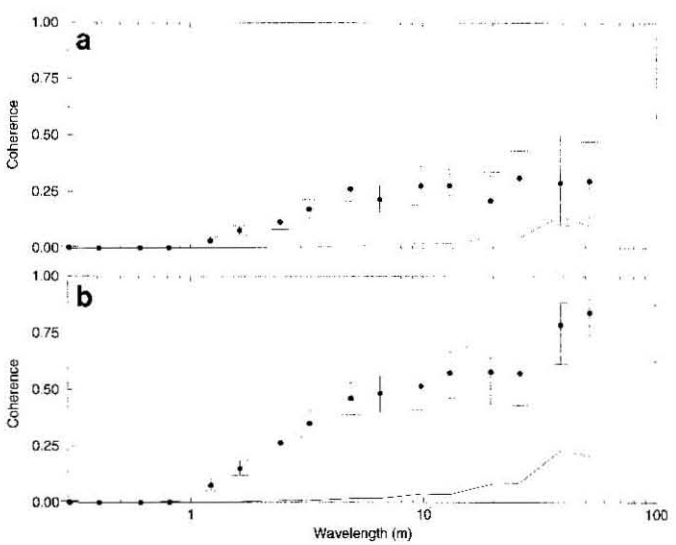

Figure 12. Comparison of the coherences between the *Vp* and *Vs* logs for the (a) gneiss and (b) metabasite sequences defined in Tables 1 and 2. The error bars are 95% confidence intervals, and the solid line is the 95% confidence interval for two incoherent series.

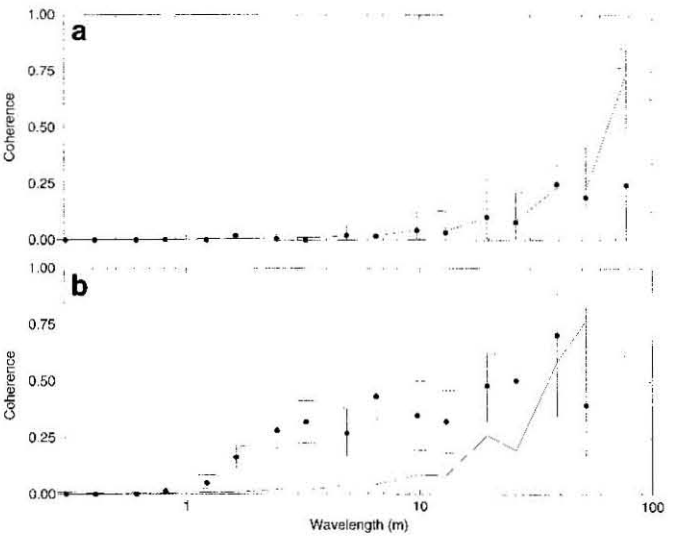

Figure 13. Comparison of the coherences between the density and *Vp* logs for the (a) gneiss and (b) metabasite sequences defined in Tables 1 and 2. The error bars are 95% confidence intervals, and the solid line is the 95% confidence interval for two incoherent series.

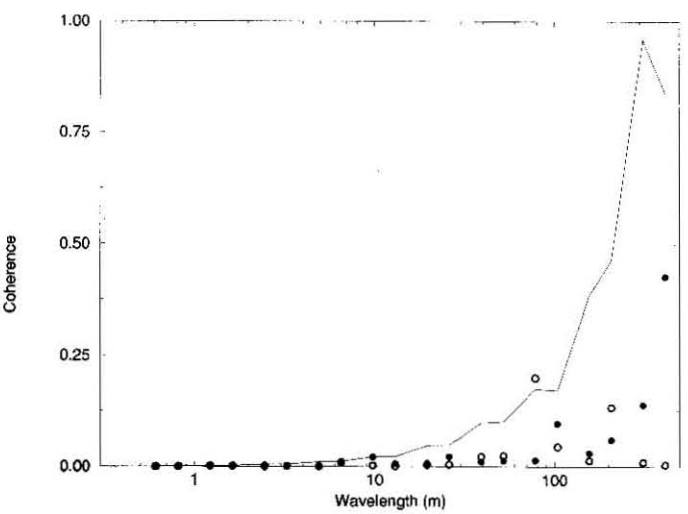

Figure 14. Coherences between the *Vp* logs for the main and pilot holes. The solid circles are for no offset between the two holes, whereas the open circles are for a vertical offset of the main hole of 550 m compared to the pilot hole to account for the 200 m hole separation and the measured 70° structural dip. The solid line is the 95% confidence interval for two incoherent series. Note that the estimates fall far below the solid line for all wavelengths.

velocity variations, whereas for the metabasites there is a significant correlation.

Interhole Coherence

The question arises whether there are any statistically significant coherences between respective logs of the pilot and main holes. This problem was previously addressed by *Wu et al.* [1994] for the *Vp* logs who, through forward modeling of the measured cross-correlation function, inferred an aspect ratio (horizontal/vertical correlation scale) of 2 to 3 for the spatial structure of seismic heterogeneity. The *Vp-Vp* coherences, for zero and 550 m vertical offset (3609 points) of the main hole *Vp* log with the pilot hole *Vp* log, are illustrated in Figure 14. Zero vertical offset assumes no structural dip and allows comparison with the results of *Wu et al.* [1994], whereas a vertical offset of 550 m attempts to align the logs from the two holes 200 m apart given the reported average structural dip of about 70° [*Franke*, 1989]. The coherence between the two logs is at the level one would expect from two totally uncorrelated data series. Similar results were obtained when the *Vs-Vs* and density-density coherences were computed. Also, none of the coherences computed between the lithologically defined subsets, e.g., {G1V, G1H}, {M1V, M1H}, {G2V ,G2H}, etc., were statistically above the 95% random correlation level.

Accordingly, we conclude that there is no statistically resolvable correlation between the sonic logs from the pilot hole with those from the main hole. This result differs from the conclusion of *Wu et al.* [1994], and we ascribe their interpretation to insufficient degrees of freedom at long wavelengths resulting in a large bias for the correlation estimator. We have not taken non-linear heterodynicity into account (stretching and compressing the logs to account for thickening and thinning of lithological units between the two holes), but on the assumption that such effects mainly distort the phase spectrum, we conclude that our results imply that the horizontal correlation scale of the velocity fluctuations is likely to be of the same order as the vertical correlation scale (~100 m). In conjunction with the statistical uniformity of upper crustal sonic logs [*Holliger*, 1996a], the implied quasi-isotropic spatial structure of seismic heterogeneity is important to studies of seismic scattering in the upper crystalline crust [*Holliger*, 1997].

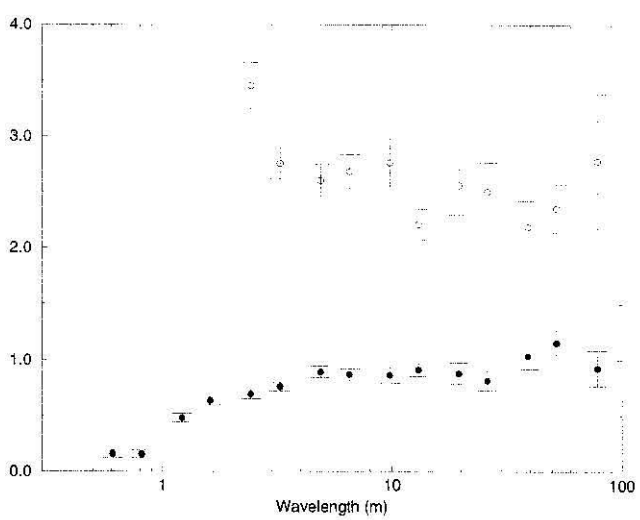

Figure 15. The real part of the transfer function between the *Vs* and *Vp* logs. The solid circles assume that the *Vs* logs are noise-free, whereas the open circles assume that the *Vp* logs are noise free. The error bars are 95% confidence intervals.

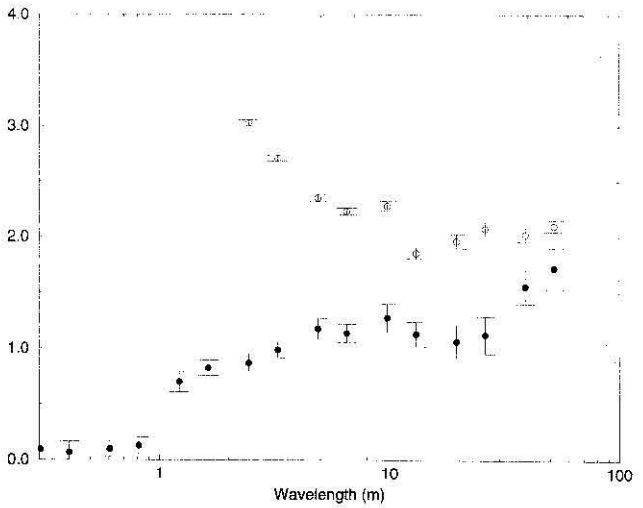

Figure 16. The real part of the transfer function between the *Vs* and *Vp* logs for the metabasite sequences only from the pilot hole (see Table 1). The solid circles assume that the *Vs* logs are noise-free, whereas the open circles assume that the *Vp* logs are noise free. The error bars are 95% confidence intervals.

Vp-Vs Transfer Function

The linear relationship between two time (or space) series can be described in the frequency (or wavenumber) domain by the complex transfer function between them, which is the analogue to the time (or space) domain impulse response function [e.g., *Jenkins and Watts*, 1968, Chapter 10; *Bendat and Piersol*, 1971, Chapter 5; *Brillinger*, 1981, Chapter 6]. For an ideal solid, the transfer function between the *Vp* and *Vs* logs should be real valued and wavenumber independent. Departures from this reflect heterogeneity variations in bulk properties that scale with wavelength, such as crack density or compositional layering. Transfer function estimates thus complement inferred spectral coherences between the sonic and density logs. The robust estimation of transfer functions is described in *Chave et al.* [1987, pp. 641-643].

The real part of the complex wavenumber domain transfer function between *Vp* and *Vs*, determined using all the data from both logs, is illustrated in Figure 15. The imaginary part of the transfer function (not shown) is statistically equal to zero, as expected. The transfer function has been estimated twice, once assuming that *Vs* is noise-free, and the other assuming that *Vp* is noise-free. The former results in downward biased estimates of the transfer function (solid circles), whereas the other results in upward biased estimates (open circles) [e.g., *Jones*, 1980]. These noise bias errors were known in many fields early this century, notably econometrics [*Gini*, 1921], but were not appreciated in geophysics until much later [e.g., *Sims et al.*, 1971]. Note that although the random error, as expressed by the 95% confidence intervals, is small, the bias error, expressed by the separation between the two estimates, is large, implying large effects due to contributions from noise autopowers. Given the generally low coherence between these series

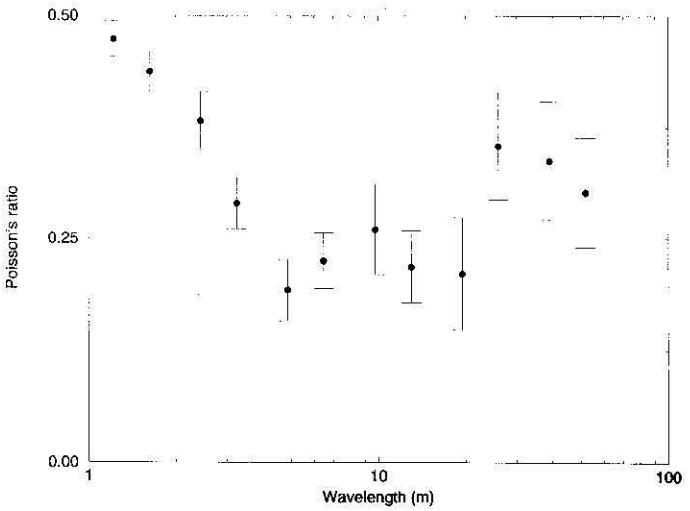

Figure 17. Poisson's ratio computed from the upward biased real part of the transfer function between the *Vs* and *Vp* logs for the metabasite sequence M2V from the pilot hole (see Table 1).

(Figure 10), this poor result is not surprising. The estimates at shorter wavelengths either approach zero or infinity, as expected from the lower coherence (Figure 10).

To improve our estimate of the transfer function, we consider those series which show strong *Vs-Vp* coherence, namely the metabasite sequences (Figure 12b). The real part of the two estimates of the transfer functions are shown in Figure 16, and there is less bias effect, but the estimates are still not useful. Note that we can reject estimates of the transfer function below 1.414, as they will lead to unphysical values for Poisson's ratio less than zero, so all the downward biased estimates are rejected on physical grounds. These estimates are too low because of the high noise on *Vs* compared to *Vp*. Using the density log as a remote reference [*Reiersøl*, 1941; *Geary*, 1943; *Goubau et al.*, 1978] to avoid noise autopowers gives estimates statistically identical to the upward biased ones, which suggests that these estimates are far less affected by noise bias than the downward biased ones.

The metabasite sequences in the pilot hole show the largest coherence between *Vp* and *Vs*. Deriving the upward biased transfer function estimates from those logs, and converting the ratios to Poisson's ratio, gives the values shown in Figure 17. Estimates at wavelengths shorter than 3 m are poor due to the low signal-to-noise ratio resulting in a large upward bias from the noise autospectra. The values for wavelengths between 3 and 60 m are physically reasonable and imply that there is a wavelength-dependent variation in Poisson's ratio, with smaller values at shorter wavelengths (3-20 m) compared to longer wavelengths (30-60 m). A histogram of point estimates of Poisson's ratio from the *Vp* and *Vs* logs in the pilot hole metabasite sequences is approximately Gaussian-like with a mean and median of 0.26, a mode of 0.275, a standard error of 0.025, and a 95% confidence interval of 0.21-0.31. These ranges are commensurate with the spectral estimates shown on Figure 17.

Discussion

Leary [1991] obtained comparable results to this study when cross-correlating sonic and resistivity logs with gamma logs from the Cajon Pass borehole. Gamma logs are primarily sensitive to petrology whereas resistivity logs are governed by pore fluids. Since the primary porosity in the probed gneissic rocks is very low, *Leary* [1991] argued that fluid-filled cracks and fractures rather than the petrology dominate the small-scale seismic structure in the upper crystalline crust. *Holliger* [1996a] found sonic logs from a wide variety of upper crusts to be surprisingly uniform in terms of their second-order statistics. Such uniform statistical properties of upper crustal velocity fluctuations are indeed consistent with the correspondingly uniform scaling laws for brittle faults and associated crack haloes [*Holliger*, 1996b]. In the following, we shall therefor explore how compatible our observations are with the interpretation that small-scale fluctuations in upper crustal velocity are dominated by cracks and their level of fluid saturation.

In an ideal solid, the relations between density and compressional and shear velocities are independent of length. The effects of dry and saturated cracks on the bulk and shear moduli are quantified, for example, in *Bourbié et al.* [1987, p. 180]. Our coherence measurements show no coherence between *Vs* and density logs, emerging coherence between *Vp* and density logs at larger wavelengths (>50 m), and weak, but significant coherence between *Vp* and *Vs* logs (Figs. 10 and 11). Cracks have dramatic effects on seismic velocities while barely affecting the density due to the low increase in total pore space. Dry cracks similarly affect the bulk and shear moduli, whereas fluid-filled cracks have only minor effects on the bulk modulus [*Bourbié et al.*, 1987, p. 180]. Fluid-filled cracks are thus indeed a possible explanation for the lack of coherence between the *Vs* and density logs. Evidently, this explanation is also consistent with reasonable coherence between the *Vp* and *Vs* logs as well as with the weak coherence between the *Vp* and density logs. The enhanced coherence between the *Vp* logs and the density and gamma logs at longer wavelengths (>50 m) (Figs. 9 and 11) might imply that at larger scales the effect of cracks diminishes and the influence of composition on velocities and densities increases, which is also the implication from the results of Poisson's ratio determination. The transition from dominantly physically controlled to dominantly compositionally controlled upper crustal structure could be related to the uniform outer range of self-affine scaling typical of upper crustal *Vp* logs [*Holliger*, 1996a].

For the lithologically defined subsets, *Vp-Vs* coherence is stronger for the metabasites than for the gneisses, and density-velocity coherence is significant for the metabasites but not for the gneisses (Figures 12 and 13). If, as speculated above, the coherence between seismic velocities and densities is governed by fluid-filled cracks, this could imply differing crack-densities and/or differing levels of fluid saturation within the gneisses and metabasites. Alternatively, differences in *Vp-Vs* and velocity-density coherences between the gneisses and metabasites could be due to differences in *Vp* and *Vs* anisotropy. However, laboratory measurements indicate that although gneisses tend to be much more anisotropic than metabasites, the respective *Vp* and *Vs* anisotropies generally agree within a few percent [*Burlini and Fountain*, 1993].

Attempts to define a transfer function between the *Vp* and *Vs* logs met with limited success, but suggest that the method may hold promise. Noise contributions were too large for all but the most coherent subsets, i.e., the metabasites in the pilot hole. Expressing the transfer function in terms of Poisson's ratio indicates that there may be a length-dependent scaling of Poisson's ratio, with increasing values at longer wavelengths. The inferred scale-dependence of the *Vp/Vs* ratio (Figs. 15, 16,

17) could be due to the stronger correlation of *Vp*, but not *Vs*, with rock chemistry at larger wavelengths as evidenced by the correlations between the velocity and gamma logs (Figure 9). Alternatively, it could reflect the presence, distribution, and level of saturation of cracks. Dry cracks are not expected to change the *Vp/Vs* ratio, whereas for saturated cracks the relationship becomes strongly nonlinear [*Bourbié et al.*, 1987]. The presence of statistically distributed saturated cracks alone can thus be expected to introduce some wavelength dependence of Poisson's ratio [Holliger, 1996a]. The observed variation of Poisson's ratio with wavelength serves a caution to those who compare laboratory determinations of Poisson's ratio on rock samples representative of a region to crustal scale seismic determinations.

Since our results corroborate the importance of fluid-filled cracks on upper crustal sonic and density logs, the question arises as to the extent that cracks are induced by the drilling process. Evidently, drilling could be expected to produce excavation damage zones that are consistent between similar rocks types. This could explain surprisingly uniform statistics of sonic logs from crystalline rocks as well as the differences between paragneisses and metabasites resolved in this study. *Holliger* [1996a] found that logging the same borehole with sonic tools with short (1 m) and long (3 m) source-receiver spacings resulted in statistically indistinguishable measurements. This suggests that either the excavation damage zone is thin and does not affect sonic log measurements significantly, or that it is very thick and completely dominates sonic log measurements. Results of high-resolution tomographic imaging of borehole walls in sedimentary rocks indicate that the latter is much less likely [*Hornby*, 1993].

Although this study was limited to logs from the KTB boreholes, the results obtained could have implications for our understanding of upper crustal structure in general. While pointing to interesting deviations in detail, robust spectral analyses of KTB logs confirm the statistical uniformity of upper crustal velocity and density fluctuations, and support the interpretation of this phenomenon in terms of fluid-filled cracks [*Leary*, 1991; *Holliger*, 1996a,c]. Of the particular importance in this context are the exceptional length of the KTB logs and the fact that the there do not seem to be any systematic statistical differences between the shallower and deeper parts of the logs. Therefore, it is plausible that the statistical uniformity of upper crustal structure suggested by sonic log measurements [*Holliger*, 1996a,b,c] can be extrapolated throughout large portions of the upper crystalline crust. Sonic and density logs do not contain any information about the spatial structure of upper crustal heterogeneity. Yet, by measuring the coherence between the pilot and main holes, which are some 200 m apart, we are able to conclude that the horizontal correlation length of the heterogeneities is certainly shorter than 200 m. It is important to point out that the certainty of this statement is entirely due to the use of robust spectral methods and corresponding error and significance estimates. Given the uniformity of upper crustal velocity fluctuations [*Holliger*, 1996a,c], the thus inferred quasi-isotropic structure is not necessarily restricted to the KTB area but could be representative of the upper crust in general, which has profound implications for seismic wave propagation [*Holliger*, 1997].

Conclusions

We have used robust methods with nonparametric error estimation to investigate the spectral properties of the sonic and density logs from the KTB deep drill holes in southeastern Germany. In addition to power spectra, we also investigated coherences between individual logs as well as between lithologically defined subsets of the logs. The power spectra generally show a 1/wavenumber decay in the intermediate wavelength range (~3-150 m), as determined by previous parametric estimates. The nonparametric approach allows resolution of deviations from this behavior at shorter and longer wavelengths, as well as between the *Vp* logs from the main and pilot holes. Whereas spectra at shorter wavelengths (<3 m) are heavily affected by filtering effects of the logging process, changes at longer wavelengths (>150 m) point to fundamental changes in the origins of density and velocity fluctuations.

Coherences between the full logs were found to be strong between *Vp* and *Vs* logs, moderate between *Vp* and density logs, and weak to insignificant between *Vs* and density logs. Statistically significant coherence was found neither between any of the physical logs and the caliper logs nor between the *Vs* logs and the gamma logs. Weak but significant coherence exists between *Vp* logs and gamma logs for wavelengths in excess of some 50 m. These results indicate that breakouts and uneven relief of the borehole wall contribute mostly to the quasi-white portions of the log spectra and that velocity and density fluctuations are governed by the physical state rather than by the petrology of the probed rocks. Analyses of the lithologically defined subsets point to significant differences in the spectral characteristics and coherences of the paragneisses and metabasites, which are not resolved analyzing the full logs or using parametric methods. No coherence was found between logs from the pilot and main holes, which may be indicative of a quasi-isotropic spatial structure. Poisson's ratio for the metabasites in the pilot hole show a wavelength-dependent variation, with lower values (0.22 ±0.025) at short wavelengths (4-20 m) compared to higher values (0.33 ±0.026) at longer wavelengths (20-60 m).

Our preferred interpretation, which is compatible with all the above observations, is that at wavelengths shorter than some 100 m, fluctuations of sonic logs are dominated by fluid-filled cracks and largely independent on the petrology of the probed rocks. Differing coherences between densities and velocities in the metabasites and paragneisses would then be indicative of differing crack densities, crack geometries, or fluid saturation. The above hypothesis could be tested by extending type of analysis presented in this paper to additional types of logs, in particular nuclear logs and/or by laboratory measurements of crack densities and geometries.

Acknowledgments. We thank Alan Chave for providing his latest robust processing codes, and Don White and Dave Eaton for fruitful discussions and thorough in-house reviews. This manuscript greatly profited from critical comments and suggestions by Volker Haak and two anonymous referees. Sonic, density and caliper logs were provided by KTB project management, gamma logs were provided by Roland Gritto. Geological Survey of Canada contribution 42195, ETH-Geophysics contribution 924.

References

Bendat, J.S., and A.G. Piersol, *Random Data*, 407 pp., John Wiley, New York, 1971.

Bourbié, T., O. Coussy, and B. Zinszner, *Acoustics of Porous Media*, 352 pp., Gulf Publ., Houston, Tex., 1987.

Brillinger, D.R., *Time series data analysis and theory (Expanded edition)*, 540 pp., Holden-Day, Merryfield, Va., 1981

Burke, M.M., and D.M. Fountain, Seismic properties of rocks from an

exposure of extended continental crust- New laboratory measurements from the Ivrea Zone, *Tectonophysics, 182*, 119-146, 1990.
Burlini, L., and D.M. Fountain, Seismic anisotropy of metapelites from the Ivrea-Verbano zone and Serie dei Laghi (northern Italy), *Phys. Earth Planet. Inter., 78*, 301-317, 1993.
Chave, A.D., and D.J. Thomson, Some comments on magnetotelluric response function estimation, *J. Geophys. Res., 94*, 14,215-14,225, 1989.
Chave, A.D., D.J. Thomson, and M.E. Ander, On the robust estimation of power spectra, coherences, and transfer functions. *J. Geophys. Res., 92*, 633-648, 1987.
Dyck, A.V., Borehole geophysics applied to metallic mineral prospecting: A review, *Pap. Geol. Surv. Can., 75*(31), 65 pp., 1975.
Efron, B., The Jackknife, the Bootstrap, and other resampling plans, 92 pp., Soc. for Ind. and Appl. Math., Philadelphia, Pa., 1982.
Egbert, G.D., and J.R. Booker, Robust estimation of geomagnetic transfer functions, *Geophys. J. R. Astron. Soc., 87*, 173-194, 1986.
Franke, W., The geological framework of the KTB drill site, Oberpfalz, in *The German Continental Deep Drilling Program (KTB)*, edited by R. Emmermann and J. Wohlenberg, pp. 37-54, Springer-Verlag, New York, 1989.
Geary, R.C., Relations between statistics: The general and the sampling problem when the samples are large, *Proc. R. Irish Acad., 49*, 177-196, 1943.
Gini, C., Sull'interpolazione di una retta quando i valori della variabile indipendente sono affetti da errori accidentali, *Metron, 1*, 63-82, 1921.
Goubau, W.M., T.D. Gamble, and J. Clarke, Magnetotelluric data analysis: Removal of bias, *Geophysics, 43*, 1157-1166, 1978.
Green, A.G., and J.A. Mair, Subhorizontal fractures in a granitic pluton: Their detection and implications for radioactive wave disposal, *Geophysics, 48*, 1428-1449, 1983.
Hampel, F.R., E.M. Ronchetti, P.J. Rousseeuw, and W.A. Stahel, *Robust Statistics*, 502 pp., John Wiley, New York, 1986.
Hansen, B.T., S. Teufel, and H. Ahrendt, Geochronology of the Moldanubian-Saxothuringian transition zone, northeast Bavaria, in *The German Continental Deep Drilling Program (KTB)*, edited by R. Emmermann and J. Wohlenberg, pp. 55-65, Springer-Verlag, New York, 1989.
Hoaglin, D.C., F. Mosteller, and J.W. Tukey, *Understanding Robust and Exploratory Data Analysis*, 447 pp., John Wiley, New York, 1983.
Holliger, K., Upper crustal seismic velocity heterogeneity as derived from a variety of P-wave sonic logs, *Geophys. J. Int., 125*, 813-829, 1996a.
Holliger, K., Fault-scaling and $1/f$ noise properties of seismic velocity fluctuations in the upper crystalline crust, *Geology*, 24, 1103-1106, 1996b.
Holliger, K., Seismic scattering in the upper crystalline crust based on evidence from sonic logs, *Geophys. J. Int.*, 128, 65-72, 1997.
Holliger, K., A.G. Green, and C. Juhlin, Stochastic analysis of sonic from the upper crystalline crust: Methodology, *Tectonophysics*, 264, 341-356, 1996.
Hornby, B.E., Tomographic reconstruction of near-borehole slowness using refracted borehole sonic arrivals, *Geophysics, 58*, 1726-1738, 1993.
Huber, P.J., *Robust Statistics*, 308 pp., John Wiley, New York, 1981.
Jones, A.G., Transformed coherence functions for multivariate studies, *IEEE Trans. Acoust. Speech Signal Process., 29*, 317-319, 1979.
Jones, A.G., Geomagnetic induction studies in Scandinavia, I, Determination of the inductive response function from the magnetometer array data. *J. Geophys., 48*, 181-194, 1980.
Jones, A.G., and H. Jödicke, Magnetotelluric transfer function estimation improvement by a coherence-based rejection technique, paper presented at 54th Annual Society for Exploration Geophysicists Meeting, Atlanta, Ga., Dec. 2-6, 1984.
Jones, A.G., A.D. Chave, G. Egbert, D. Auld, and K. Bahr, A comparison of techniques for magnetotelluric response function estimation, *J. Geophys. Res., 94*, 14,201-14,213, 1989.
Kneib, G., The statistical nature of the upper continental crystalline crust derived from in-situ seismic measurements, *Geophys. J. Int., 122*, 594-616, 1995.
Leary, P.C., Deep borehole evidence for fractal distribution of fractures in crystalline rock, *Geophys. J. Int., 107*, 615-627, 1991.
Milkereit, B., A. Green, J. Wu, and E. Adam, Integrated seismic and borehole study of the Sudbury igneous complex, *Geophys. Res. Lett., 21*, 931-934, 1994.
Nuttall, A.H., and G.C. Carter, Bias of the estimate of the magnitude-squared coherence, *IEEE Trans. Acoust. Speech Signal Process., 24*, 582-583, 1976.
Owens, A.J., On the detrending and smoothing of data, *J. Geophys. Res., 83*, 221-224, 1978.
Reiersøl, O., Confluence analysis by means of lag moments and other methods of confluence analysis, *Econometrica, 9*, 1-22, 1941.
Silver, L.T., and E.W. Jame, Geologic setting and lithologic column of the Cajon pass deep drill hole, *Geophys. Res. Lett., 15*, 941-944, 1988.
Sims, W.E., F.X. Bostick, and H.W. Smith, The estimation of magnetotelluric tensor elements from measured data, *Geophysics, 36*, 938-942, 1971.
Slepian, D., Prolate spheroidal wavefunctions, Fourier analysis, and uncertainty, V, The discrete case, *Bell Syst. Tech. J., 57*, 1371-1429, 1978.
Thomson, D.J., Spectrum estimation techniques for characterization and development of WT4 waveguide, I, *Bell Syst. Tech. J., 56*, 1769-1815, 1977a.
Thomson, D.J., Spectrum estimation techniques for characterization and development of WT4 waveguide, II, *Bell Syst. Tech. J., 56*, 1983-2005, 1977b.
Thomson, D.J., Spectrum estimation and harmonic analysis, *Proc. IEEE, 70*, 1055-1096, 1982.
Thomson, D.J., and A.D. Chave, Jackknife error estimates for spectra, coherences, and transfer functions, in *Advances in Spectral Analysis and Array Processing*, edited by S. Haykin, pp. 58-113, Prentice-Hall, Englewood Cliffs, N.J., 1991.
Todoeschuck, J.P., and O.G. Jensen, Joseph geology and seismic deconvolution, *Geophysics, 53*, 1410-1414, 1988.
Walden, A.T., and J.W.J. Hosken, An investigation of the spectral properties of primary reflection coefficients, *Geophys. Prospect., 33*, 400-435, 1985.
Wu, R.-S., Z. Xu, and X.-P. Li, Heterogeneity spectrum and scale-anisotropy in the upper crust revealed by the German continental deep-drilling (KTB) holes, *Geophys. Res. Lett., 21*, 911-914, 1994.

K. Holliger, Institute of Geophysics, Swiss Federal Institute of Technology, ETH-Hönggerberg, CH-8093 Zurich, Switzerland. (email: klaus@augias.geo.phys.ethz.ch)

A.G. Jones, Geological Survey of Canada, 1 Observatory Crescent, Ottawa, Ontario, Canada, K1A 0Y3. (email: jones@cg.NRCan.gc.ca)

(Received February 5, 1996; revised August 1, 1996;
accepted November 21, 1996.)